



Cite this: *RSC Adv.*, 2020, **10**, 45112

Received 2nd November 2020  
 Accepted 10th November 2020

DOI: 10.1039/d0ra09307f  
[rsc.li/rsc-advances](http://rsc.li/rsc-advances)

## Selective complexation and efficient separation of *cis/trans*-1,2-dichloroethene isomers by a pillar[5]arene†

Bin Li, <sup>ab</sup> Kaidi Xu,<sup>a</sup> Yiliang Wang, <sup>a</sup> Hang Su,<sup>a</sup> Lei Cui<sup>a</sup> and Chunju Li <sup>ab</sup>

The complexation and separation of industrially important *cis*- and *trans*-1,2-dichloroethene (*cis*- and *trans*-DCE) isomers using perethylated pillar[5]arene (EtP5) are described. EtP5 exhibits considerable binding capability for the *trans*-DCE isomer over the *cis*-DCE in organic solution. Furthermore, nonporous adaptive crystals (NACs) of EtP5 can efficiently separate *trans*-DCE from a 50 : 50 (v/v) *cis*-*trans*-isomer mixture.

1,2-Dichloroethenes (DCEs), including *cis*-DCE and *trans*-DCE isomers, are high-value chemicals with a variety of uses in synthetic chemistry and chemical industry.<sup>1</sup> They are widely applied as low-temperature extraction solvents for heat sensitive substances and feedstocks for synthesizing copolymer materials with other unsaturated monomers.<sup>2</sup> *trans*-DCE and *cis*-DCE can be also used as an environment-friendly refrigerant and foaming additive agent, respectively. In the industrial production process, they are produced as a mixture of *cis* and *trans*-DCE isomers by direct chlorination of acetylene or by the pyrolytic dehydrochlorination of 1,1,2-trichloroethane.<sup>3</sup> In most cases, the two isomers must be used separately. However, the separation of *cis*- and *trans*-DCE isomers is difficult due to their similar molecular sizes and close boiling points. Industrially, although both isomers can be separated by fractional distillation with very high columns, this process is high energy-consumption and environmentally unfriendly.

Crystalline porous materials such as zeolites,<sup>4,5</sup> metal-organic frameworks (MOFs)<sup>6–9</sup> and covalent organic frameworks (COFs)<sup>10</sup> have been described as promising adsorbents for the economical and energy-efficient separation of hydrocarbons (e.g., alkanes, alkenes and benzene derivatives). However, the examples of the physisorptive separation of *cis*- and *trans*-isomers are relatively scarce.<sup>11–14</sup> Recently, a novel class of macrocycle-based crystalline materials, termed as nonporous adaptive crystals (NACs) of pillar[*n*]arenes, has shown

interesting adsorption/separation properties.<sup>15–21</sup> Subsequently, some new NACs based on other important macrocycles<sup>22</sup> such as biphen[*n*]arene,<sup>23</sup> leaning towerarene,<sup>24,25</sup> tiararene,<sup>26</sup> geminiarene,<sup>27</sup> hybrid[3]arene,<sup>28</sup> naphthotubes<sup>29</sup> and cucurbit[6]uril<sup>30</sup> have been developed. In comparison with traditional porous materials, which usually possess large surface area, NACs are nonporous and structurally adaptive in the initial crystalline state. The intrinsic or extrinsic porosity inside macrocycle crystals could be opened by capturing preferable vaporized molecules, forming corresponding host-guest crystal structures along with a solid-state structural transformation. This unique feature enables NACs to work as adsorptive materials in adsorption and separation at the solid-vapor phase.

Very recently, our group used NACs of 2,2',4,4'-biphen[3]arene (MeBP3 $\alpha$ ) to separate *cis*-DCE from *trans*-DCE with a purity of 96.4% in the solid-vapor state.<sup>23</sup> Crystal structure of *cis*-DCE@MeBP3 reveals that *cis*-DCE molecules are not encapsulated into macrocycle cavities, but located in self-assembled extrinsic porosity. Here, we present that perethylated pillar[5]arenes (EtP5) display a totally opposite selectivity to preferentially bind *trans*-DCE over its *cis*-isomer not only in solution but also in the solid state. The selectivity comes from the suitability of size/shape between EtP5's cavity and *trans*-DCE. NACs of EtP5 (EtP5 $\alpha$ ) efficiently separate *trans*-DCE from the 50 : 50 (v/v) mixture of *cis/trans*-DCE isomers with 94.94% purity (Fig. 1), accompanied by adsorption induced crystalline structure transformation. More intriguingly, when EtP5 $\alpha$  and MeBP3 $\alpha$  are exposed to *cis*- and *trans*-DCE mixed vapor, they exhibit self-sorting adsorption behavior for the two isomers, *i.e.* producing *trans*-DCE@EtP5 and *cis*-DCE@MeBP3.

As we know, pillar[*n*]arenes, as important family of supramolecular macrocycles with prism-like geometries and  $\pi$ -rich cavities, have shown interesting cavity host-guest properties towards a variety of guest molecules.<sup>31–41</sup> The most peculiar complexation behavior of pillar[*n*]arenes is that pillar[5]arenes

<sup>a</sup>College of Science, Center for Supramolecular Chemistry and Catalysis, Shanghai University, Shanghai 200444, P. R. China. E-mail: [cjli@shu.edu.cn](mailto:cjli@shu.edu.cn)

<sup>b</sup>Key Laboratory of Inorganic-Organic Hybrid Functional Material Chemistry, Ministry of Education, Tianjin Key Laboratory of Structure and Performance for Functional Molecules, College of Chemistry, Tianjin Normal University, Tianjin 300387, P. R. China

† Electronic supplementary information (ESI) available:  $^1\text{H}$  NMR spectra, NMR titration curves, single crystal data and vapor adsorption. CCDC 2025010 and 1905571. For ESI and crystallographic data in CIF or other electronic format see DOI: 10.1039/d0ra09307f



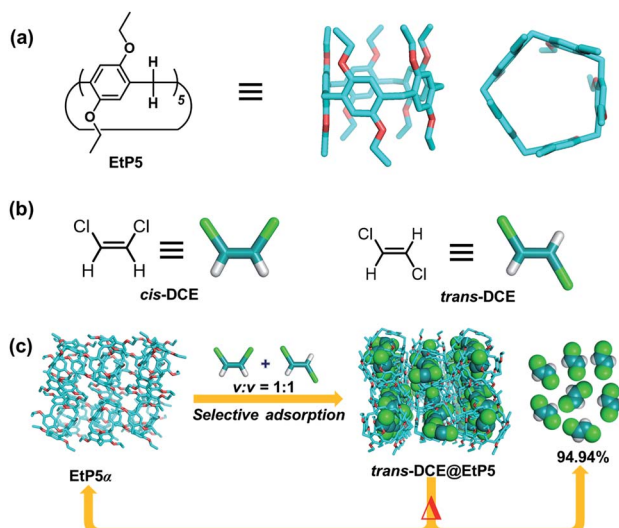


Fig. 1 Chemical structures of (a) EtP5 and (b) *cis*-DCE and *trans*-DCE. (c) Schematic representation of the *cis*/*trans*-DCE isomers separation and the structural transformation.

can strongly bind suitable neutral molecules in organic solution compared with other popular macrocycles.<sup>42–46</sup>

First, we tested the host–guest complexation between *cis*- or *trans*-DCE and EtP5 in solution by <sup>1</sup>H NMR spectroscopy (Fig. S1 and S2, ESI†). As shown in Fig. 2, when equimolar EtP5 was added into an *o*-xylene-*d*<sub>10</sub> solution containing *cis*- or *trans*-DCE (5.0 mM), the signal related to the protons on *trans*-DCE exhibits a very significant upfield shift of  $-0.52$  ppm as well as an extensive broadening effect compared with the free *trans*-DCE. The reason is that *trans*-DCE molecule was encapsulated in the cavity of EtP5 forming a threaded structure. Simultaneously, the aromatic protons on EtP5 moved downfield with slight chemical shift as a result of the interactions with *trans*-DCE. However, no obvious signal changes were observed when *cis*-DCE and EtP5 were mixed in *o*-xylene-*d*<sub>10</sub>, suggesting that *cis*-

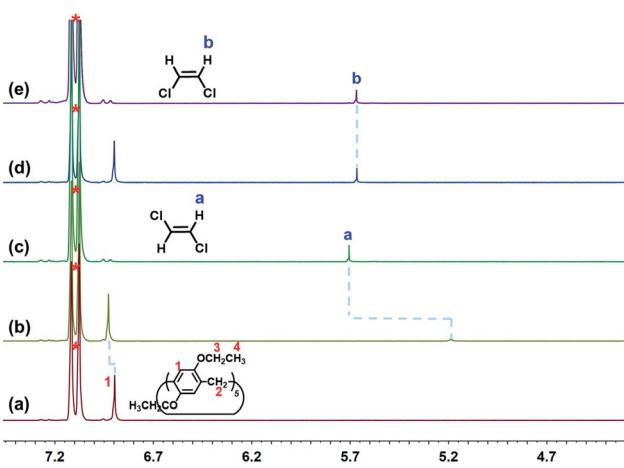


Fig. 2 Partial proton <sup>1</sup>H NMR spectra (500 MHz) of (a) EtP5, (b) EtP5 + *trans*-DCE, (c) *trans*-DCE, (d) EtP5 + *cis*-DCE, and (e) *cis*-DCE at 5.0 mM in *o*-xylene-*d*<sub>10</sub>.  $\ast$  indicates the solvent peaks.

DCE can not be contained in the cavity of EtP5. *trans*-DCE molecule with stretched structure is more suitable for the cavity of EtP5.<sup>45</sup> It was observed that the inclusion-induced upfield shift of *trans*-DCE ( $\Delta\delta = -0.25$  ppm for H<sub>a</sub>) in CDCl<sub>3</sub> was smaller than those observed in *o*-xylene-*d*<sub>10</sub> (Fig. S3 and S4, ESI†), suggesting that stronger host–guest interactions occurred in the non-polar *o*-xylene-*d*<sub>10</sub> solution. For comparison purpose, the interaction between perethylated pillar[6]arene (EtP6) and *cis*- or *trans*-DCE was also investigated. No obvious complexation was detected (Fig. S5 and S6, ESI†), which is reasonable that the guests are too small in comparison with EtP6's cavity. To determine the binding affinity of EtP5 to *trans*-DCE, <sup>1</sup>H NMR titration methods were employed with the concentration of EtP5 kept constant at 0.50 mM and that of *trans*-DCE varied from 0 to 33.8 mM in *o*-xylene-*d*<sub>10</sub> (Fig. S7, ESI†). The association constant ( $K_a$ ) was determined to be  $(1.03 \pm 0.12) \times 10^2$  M<sup>-1</sup> by a nonlinear curve-fitting method, which is larger than that in CDCl<sub>3</sub> ( $31.5 \pm 4.1$  M<sup>-1</sup>, Fig. S8, ESI†).

X-ray crystallography further confirmed the formation of inclusion complex. Crystals of *trans*-DCE@EtP5 were successfully obtained by slow evaporation of a solution of EtP5 in *trans*-DCE (Table S1, ESI†). The crystal structure of *trans*-DCE@EtP5 is shown in Fig. 3a and S9.† One *trans*-DCE molecule threads through the cavity of EtP5 to form an inclusion complex in the solid state, which is stabilized by triple C–H···π forces and triple weak C–H···Cl interactions (Fig. S10, ESI†). In addition, in the stacking mode of *trans*-DCE@EtP5, we find extra *trans*-DCE molecules lie in the channel formed by two adjacent EtP5 molecules (Fig. S9, ESI†). Although no host–guest interactions were found between EtP5 and *cis*-DCE in solution, we attempted to grow the crystals of *cis*-DCE@EtP5. Interestingly, when EtP5 was crystallized from *cis*-DCE solution, the obtained crystal structure of EtP5 did not contain *cis*-DCE molecules and formed a new structure (Fig. 3b and Table S2†). The experimental and simulated powder X-ray diffraction (PXRD) pattern of EtP5

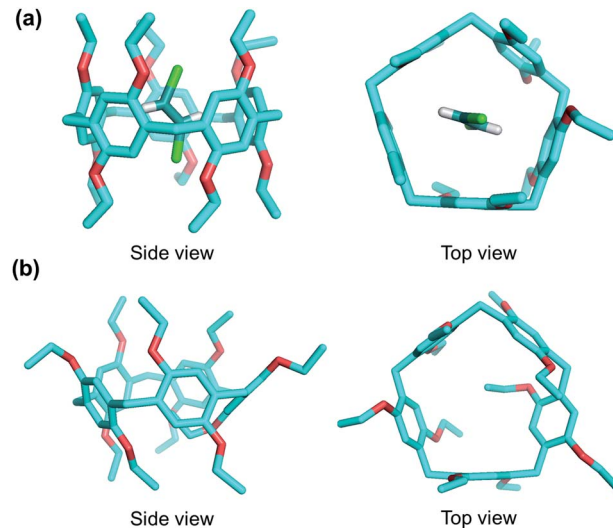


Fig. 3 Molecular structures of (a) *trans*-DCE@EtP5 and (b) *cis*-DCE-free EtP5 obtained from *cis*-DCE solution in the solid-state.



crystals crystallized in *cis*-DCE was a perfect match for EtP5 $\alpha$  (Fig. S11, ESI $\dagger$ ), suggesting that EtP5 $\alpha$  has the same structure as EtP5 crystallized in *cis*-DCE.

Based on the above highly selective host–guest complexation both in solution and in the solid state, we considered the selective adsorption of *cis*- and *trans*-DCE isomers vapor by EtP5 $\alpha$ . Single-component time-dependent solid-vapor sorption experiments were examined to test the adsorption capacity using crystalline EtP5 $\alpha$  by  $^1\text{H}$  NMR spectroscopy. As shown in Fig. S12, $\dagger$  EtP5 $\alpha$  can rapidly capture *trans*-DCE vapor with an adsorption amount of about one *trans*-DCE/EtP5 (Fig. S14, ESI $\dagger$ ). By contrast, EtP5 $\alpha$  did not take up *cis*-DCE vapor (Fig. S13 and S15, ESI $\dagger$ ). Thermogravimetric analysis (TGA) measurement was further confirmed the uptake amount of *trans*-DCE (Fig. S16, ESI $\dagger$ ). However, the single-crystal structure of *trans*-DCE@EtP5 shows two host molecules and four *trans*-DCE, which is different from the results of vapor adsorption. This could be reasonable that during the removal of physical surface adsorption before NMR and TGA measurements (for details see ESI $\dagger$ ), the guest molecules located at the outside of EtP5 were easily desorbed, while those stabilized in the cavities remained. $^{47}$

In order to investigate the mechanism for the uptake of *trans*-DCE vapor by EtP5 $\alpha$ , PXRD experiments were carried out. The PXRD pattern of EtP5 $\alpha$  after adsorption of *trans*-DCE was different from that of the EtP5 $\alpha$  but almost identical to that of the simulated pattern determined from *trans*-DCE@EtP5 (Fig. 4a), suggesting that the uptake of *trans*-DCE induces the structural transformation of EtP5 $\alpha$  into *trans*-DCE@EtP5. As expected, exposing EtP5 $\alpha$  to *cis*-DCE vapor did not result in any structure changes (Fig. 4a).

Considering the remarkable adsorption selectivity in the single-component sorption experiments, we wondered whether crystalline EtP5 $\alpha$  materials would be able to separate *trans*-DCE from *cis*-DCE. Therefore, a time-dependent EtP5 $\alpha$  solid-vapor sorption experiment for the *cis*-/*trans*-DCE (50 : 50 v/v) mixture was performed. As shown in Fig. 4b, the adsorption of *trans*-DCE in EtP5 $\alpha$  was very fast. Meanwhile, the uptake amount of *cis*-DCE by EtP5 $\alpha$  was tiny. According to gas chromatography (GC), the adsorption percentages of *trans*-DCE is up to 94.94% at the saturated adsorption point (Fig. S17, ESI $\dagger$ ). These results indicate that EtP5 $\alpha$  favors to capture *trans*-DCE over *cis*-DCE vapor from their isomers mixture. Then, we measured the recycling adsorption capacity of EtP5 $\alpha$ . After five adsorption–desorption cycles, no distinct loss of performance in the selective of the *trans*-DCE uptake was observed (Fig. S18 and S19, ESI $\dagger$ ), showing that EtP5 $\alpha$  crystals have excellent separation abilities.

Owing to the opposite adsorption selectivity for *cis*-/*trans*-DCE isomers of EtP5 $\alpha$  and MeBP3 $\alpha$ , $^{23}$  we considered the use of co-adsorbents to achieve the self-sorting discrimination of the two isomers. We then conducted the self-sorting uptake experiments (details see ESI $\dagger$ ). As expected, when exposing EtP5 $\alpha$  and MeBP3 $\alpha$  in the saturated vapor of *cis*- and *trans*-DCE (50 : 50 v/v) mixture (Fig. 4c), EtP5 $\alpha$  selectively took up *trans*-DCE, and MeBP3 $\alpha$  tended to adsorb *cis*-DCE (Fig. S20 and S22 $\dagger$ ), giving the uptake ratios of 95.27% and 93.80%, respectively (Fig. 4d, S21 and S23 $\dagger$ ).

In summary, we have demonstrated the *cis*-/*trans*-selective complexation of industrially important DCE isomers by EtP5 macrocycle both in solution and in the solid state. Its adaptive crystals, EtP5 $\alpha$ , are able to efficiently separate *trans*-DCE from a *cis*- and *trans*-DCE isomers mixture. The selectivity derives from the size/shape-fit host–guest complexation and the vapor-induced crystalline structure transformation. Interestingly, a self-sorting adsorption method to simultaneously separate *cis*- and *trans*-isomers by crystalline EtP5 $\alpha$  and MeBP3 $\alpha$  materials has been presented. Future work will attempt to achieve more separation of configurational isomers using extended biphen[n] arene $^{48}$  and functional macrocycles. $^{49}$

## Conflicts of interest

There are no conflicts to declare.

## Acknowledgements

This work was supported by NNSFC (No. 21971192 and 21772118), and funds provided by Tianjin Normal University.

## Notes and references

- 1 K. A. Marshall, Chlorocarbons and Chlorohydrocarbons, Survey, *Kirk-Othmer Encyclopedia of Chemical Technology*, Wiley-Interscience, New York, 2003.
- 2 F. Richter, *Beilsteins Handbuch der organischen Chemie*, EIII, 1958, vol. 1, p. 652.
- 3 J. W. Scroggins, US20070191653, 2007.

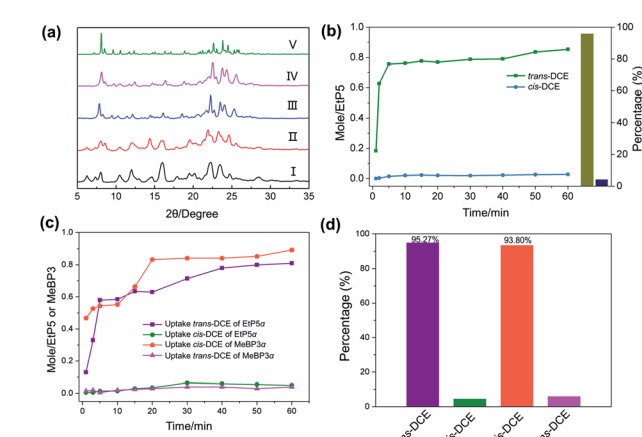


Fig. 4 (a) PXRD patterns of EtP5: (I) original EtP5; (II) after uptake of *cis*-DCE vapor; (III) after uptake of *cis*/*trans*-DCE mixed vapor; (IV) after uptake of *trans*-DCE vapor; (V) simulated from single-crystal structure of *trans*-DCE@EtP5. (b) Time-dependent vapor-solid sorption plot of EtP5 for *cis*- and *trans*-DCE (50 : 50 v/v) mixed vapor and the relative uptake ratios determined by GC. (c) Time-dependent self-sorting sorption plot of EtP5 and MeBP3 for *cis*- and *trans*-DCE (50 : 50 v/v) mixed vapor. (d) The relative uptake ratios determined by GC.



4 M. Yu, R. D. Noble and J. L. Falconer, *Acc. Chem. Res.*, 2011, **44**, 1196–1206.

5 Y. Yang, P. Bai and X. Guo, *Ind. Eng. Chem. Res.*, 2017, **56**, 14725–14753.

6 H. Furukawa, K. E. Cordova, M. O’Keeffe and O. M. Yaghi, *Science*, 2013, **341**, 1230444.

7 H. Wang and J. Li, *Acc. Chem. Res.*, 2019, **52**, 1968–1978.

8 E. D. Bloch, W. L. Queen, R. Krishna, J. M. Zadrozny, C. M. Brown and J. R. Long, *Science*, 2012, **335**, 1606–1610.

9 Z. R. Herm, E. D. Bloch and J. R. Long, *Chem. Mater.*, 2014, **26**, 323–338.

10 Y. Zhao, *Chem. Mater.*, 2016, **28**, 8079–8081.

11 L. Alaerts, M. Maes, M. A. van der Veen, P. A. Jacobs and D. E. De Vos, *Phys. Chem. Chem. Phys.*, 2009, **11**, 2903–2911.

12 H. Liu, Y. He, J. Jiao, D. Bai, D. Chen, R. Krishna and B. Chen, *Chem.-Eur. J.*, 2016, **22**, 14988–14997.

13 A. Luna-Triguero, J. M. Vicent-Luna, A. Poursaeidesfahani, T. J. H. Vlugt, R. Sánchez-de-Armas, P. Gómez-Álvarez and S. Calero, *ACS Appl. Mater. Interfaces*, 2018, **10**, 16911–16917.

14 M. Maes, L. Alaerts, F. Vermoortele, R. Ameloot, S. Couck, V. Finsy, J. F. M. Denayer and D. E. De Vos, *J. Am. Chem. Soc.*, 2010, **132**, 2284–2292.

15 K. Jie, Y. Zhou, E. Li and F. Huang, *Acc. Chem. Res.*, 2018, **51**, 2064–2072.

16 T. Ogoshi, R. Suetō, K. Yoshikoshi, Y. Sakata, S. Akine and T.-a. Yamagishi, *Angew. Chem., Int. Ed.*, 2015, **54**, 9849–9852.

17 M. Wang, J. Zhou, E. Li, Y. Zhou, Q. Li and F. Huang, *J. Am. Chem. Soc.*, 2019, **141**, 17102–17106.

18 T. Ogoshi, K. Saito, R. Suetō, R. Kojima, Y. Hamada, S. Akine, A. M. P. Moeljadi, H. Hirao, T. Kakuta and T. Yamagishi, *Angew. Chem., Int. Ed.*, 2018, **57**, 1592–1595.

19 K. Jie, M. Liu, Y. Zhou, M. A. Little, S. Bonakala, S. Y. Chong, A. Stephenson, L. Chen, F. Huang and A. I. Cooper, *J. Am. Chem. Soc.*, 2017, **139**, 2908–2911.

20 Y. Zhou, K. Jie, R. Zhao, E. Li and F. Huang, *J. Am. Chem. Soc.*, 2020, **142**, 6957–6961.

21 X. Sheng, E. Li, Y. Zhou, R. Zhao, W. Zhu and F. Huang, *J. Am. Chem. Soc.*, 2020, **142**, 6360–6364.

22 J.-R. Wu and Y.-W. Yang, *Angew. Chem., Int. Ed.*, 2020, **59**, DOI: 10.1002/anie.202006999.

23 Y. Wang, K. Xu, B. Li, L. Cui, J. Li, X. Jia, H. Zhao, J. Fang and C. Li, *Angew. Chem., Int. Ed.*, 2019, **58**, 10281–10284.

24 J.-R. Wu, B. Li and Y.-W. Yang, *Angew. Chem., Int. Ed.*, 2020, **59**, 2251–2255.

25 J.-R. Wu and Y.-W. Yang, *CCS Chem.*, 2020, **2**, 836–843.

26 W. Yang, K. Samanta, X. Wan, T. U. Thikkar, Y. Chao, S. Li, K. Du, J. Xu, Y. Gao, H. Zuilhof and A. C.-H. Sue, *Angew. Chem., Int. Ed.*, 2020, **59**, 2–8.

27 J.-R. Wu and Y.-W. Yang, *J. Am. Chem. Soc.*, 2019, **141**, 12280–12287.

28 J. Zhou, G. Yu, Q. Li, M. Wang and F. Huang, *J. Am. Chem. Soc.*, 2020, **142**, 2228–2232.

29 H. Yao, Y.-M. Wang, M. Quan, M. U. Farooq, L. P. Yang and W. Jiang, *Angew. Chem., Int. Ed.*, 2020, **59**, 19945–19950.

30 Q. Li, K. Jie and F. Huang, *Angew. Chem., Int. Ed.*, 2020, **59**, 5355–5358.

31 T. Ogoshi, S. Kanai, S. Fujinami, T.-a. Yamagishi and Y. Nakamoto, *J. Am. Chem. Soc.*, 2008, **130**, 5022–5023.

32 D. Cao, Y. Kou, J. Liang, Z. Chen, L. Wang and H. Meier, *Angew. Chem., Int. Ed.*, 2009, **48**, 9721–9723.

33 T. Ogoshi, T.-a. Yamagishi and Y. Nakamoto, *Chem. Rev.*, 2016, **116**, 7937–8002.

34 N. Song, T. Kakuta, T.-a. Yamagishi, Y.-W. Yang and T. Ogoshi, *Chem.*, 2018, **4**, 2029–2053.

35 K. Wang, J. H. Jordan, K. Velmurugan, X. Tian, M. Zuo, X.-Y. Hu and L. Wang, *Angew. Chem., Int. Ed.*, 2020, DOI: 10.1002/anie.202010150.

36 G. Yu, J. Zhou, J. Shen, G. Tang and F. Huang, *Chem. Sci.*, 2016, **7**, 4073–4078.

37 B. Li, Z. Meng, Q. Li, X. Huang, Z. Kang, H. Dong, J. Chen, J. Sun, Y. Dong, J. Li, X. Jia, J. L. Sessler, Q. Meng and C. Li, *Chem. Sci.*, 2017, **8**, 4458–4464.

38 J. Chen, H. Ni, Z. Meng, J. Wang, X. Huang, Y. Dong, C. Sun, Y. Zhang, L. Cui, J. Li, X. Jia, Q. Meng and C. Li, *Nat. Commun.*, 2019, **10**, 3546.

39 X.-B. Hu, Z. Chen, G. Tang, J. Hou and Z.-T. Li, *J. Am. Chem. Soc.*, 2012, **134**, 8384–8387.

40 Q. Hao, Y. Chen, Z. Huang, J.-F. Xu, Z. Sun and X. Zhang, *ACS Appl. Mater. Interfaces*, 2018, **10**, 5365–5372.

41 S.-H. Li, H.-Y. Zhang, X. Xu and Y. Liu, *Nat. Commun.*, 2015, **6**, 7590.

42 X. Shu, S. Chen, J. Li, Z. Chen, L. Weng, X. Jia and C. Li, *Chem. Commun.*, 2012, **48**, 2967–2969.

43 C. Li, *Chem. Commun.*, 2014, **50**, 12420–12433.

44 Y. Wang, G. Ping and C. Li, *Chem. Commun.*, 2016, **52**, 9858–9872.

45 X. Zhang, X. Wang, B. Wang, Z.-J. Ding and C. Li, *Chin. Chem. Lett.*, 2020, DOI: 10.1016/j.cclet.2020.02.037.

46 B. Li, S. Li, B. Wang, Z. Meng, Y. Wang, Q. Meng and C. Li, *iScience*, 2020, **23**, 101443.

47 W. Zhu, E. Li, J. Zhou, Y. Zhou, X. Sheng and F. Huang, *Mater. Chem. Front.*, 2020, **4**, 2325–2329.

48 B. Li, B. Wang, X. Huang, L. Dai, L. Cui, J. Li, X. Jia and C. Li, *Angew. Chem., Int. Ed.*, 2019, **58**, 3885–3889.

49 K. Xu, Z.-Y. Zhang, C. Yu, B. Wang, M. Dong, X. Zeng, R. Gou, L. Cui and C. Li, *Angew. Chem., Int. Ed.*, 2020, **59**, 7214–7218.

